Oxygen and Iron Production by Electrolytic Smelting of Lunar Soil

R. O. Colson and L. A. Haskin

Deptartment of Earth and Planetary Science and McDonnell Center for the Space Sciences

Washington University

Abstract

Our work of the past year has involved two aspects: 1) electrolysis experiments on a larger scale than we had done before and 2) collaboration with Carbotek Inc. on design for a lunar magma electrolysis cell. These are discussed more in the paragraphs below.

We have demonstrated previously that oxygen can be produced by direct electrolysis of silicate melts (Lindstrom and Haskin, 1979; Haskin et al., 1986). Previous experiments using 50-100mg of melt have succeeded in measuring melt resistivities, oxygen production efficiencies, and have identified the character of metal products (Colson and Haskin, 1990; Colson, 1990; Haskin et al., 1992). We have now completed a series of experiments using 1-8 grams of silicate melt, done in alumina and spinel containers sufficiently large that surface tension effects between the melt and the wall are expected to have minor effect on the behavior of the melt in the region of the electrodes. The purpose of these experiments was to demonstrate the durability of the electrode and container materials, demonstrate the energy efficiency of the electrolysis process, further characterize the nature of the expected metal and spinel products, measure the efficiency of oxygen production and compare to that predicted on the basis of the smaller-scale experiments, and identify any unexpected benefits or problems of the process. Four experimental designs were employed, illustrated in *Figures 1*, *2*, and *3*, with a fourth design being analogous to *Figure 2* but using spinel rather than alumina tubes. Detailed results of these experiments are given in the appendix ("Summary of scaling-up experiments"); a general report of the results is given below in terms of implications of the experiments on container materials, cathode materials, anode materials, bubble formation and frothing of the melt, cell potential, anode-cathode distance, oxygen efficiency, and energy efficiency.

Our collaboration with Carbotek Inc. included providing advice and expertise on ceramic, metal, and silicate melt behavior during electrolysis as pertains to the SBIR Phase I design of a magma electrolysis cell. This collaboration was interactive, involving several extended discussion over the phone and in person in which we provided information about relevant properties of silicate melts and offered extensive suggestions about the design of the cell, both in terms of what can be expected to work based on our experimental experience and what monitoring capabilities should be built into the experiments to allow results to be adequately understood. We also contributed suggestions for experimental measurements, procedures, and post-experimental analyses for their proposed Phase II experimental work.

Container material:

We continue to use spinel containers successfully in experiments, with no indication of chemical corrosion of the containers. However, some spinel containers contain sufficient porosity (as much as 30%) and permeability that silicate melt substantially invades the spinel wall leading to a loss of silicate from our experiments and weakened container walls. The most porous spinels appear to have substantially poorer strength characteristics as well and tend to break under the weight of the assembly itself (e.g. experiments Elecss2R, Elecss2T). We note that containers made of denser spinel show no indication of invasion by the silicate melt or of breaking during experiments. Thus, high-density spinel must be used for the electrolysis cell.

We also did several experiments (Elecss2L-Elecss2O) in higher-density alumina containers. These containers showed better strength characteristics than the high-porosity spinel and were not invaded by melt. However, the reactions Al2O3 (container) » Al2O3 (melt) and Al2O3 (container) + MgO (melt) » MgAl2O4 (spinel) (coating the inner container wall), sharply increased viscosity of the melt and decreased conductivity. Loss of Al2O3 from the wall would eventually corrode the wall as well. Thus, if alumina is found to have better strength properties than even the low-porosity spinel, it can only be used as a container if it is coated with spinel on the face contacting the melt.

Cathode design:

An attempt was made in experiments Elecss2E-Elecss2K (see *Figure 1*) to effect a solid wire connection to the molten metal cathode (Fe-Si) through a small hole in the spinel container. This failed because the connecting wire quickly melted and the connection was lost (because surface tension effects prevented the molten metal from making a connection through the small hole in the ceramic). We achieved a workable connection to the cathode in experiments Elecss2L-Elecss2T (see

Figure 2) by extending the metal cathode (we used steel) to regions of the furnace sufficiently cool that the metal does not melt. Connection to a Pt lead wire was made in this cooler region. We believe that in a scaled-up cell the connection to the Fe-Si molten pool will have to be made by some Fe-Si alloy which is cooled to keep it solid. In the highest-T parts of this lead, the molten Fe-Si alloy making up the anode pool will contact a solid metal Fe-Si alloy consisting of about 50 mole% Si (e.g. Lyman, 1973). As the lead continues to cooler regions, an iron lead may be desirable to improve conductivity (which is decreased sharply by Si); and ultimately to an even higher-conductivity material at the lowest temperatures where little diffusion occurs.

We found that the molten Fe-Si cathode pool beads strongly in spinel or alumina containers (e.g. see *Figure 4*). This beading is a serious problem in our small experiments where the tendency to bead is on a larger scale than our experiments. This beading is alleviated somewhat when the metal pool rests on a solid metal base, as in Elecss2L-Elecss2T (*Figure 2*), and may be less of a problem in larger-scale cells. Nevertheless, the constraint that cathode-anode distance be small (0.5-2cm, Colson and Haskin, 1990, Haskin et al., 1992) means that the effect of beading of the metal pool must be watched when demonstration-scale experiments are done.

Anode material:

We continue to use Pt anodes successfully. It might also be possible to use other conductors (e.g. Mo) plated with Pt to protect the metal from the corrosive melt. Although we have not tested these, such configurations have been suggested for use at oxygen-generating electrodes (Harris et al., 1985; McCullough and Marlz, 1990). We observe two events to cause the deterioration of the Pt anodes. The first is oxidation of the Pt when it remains in contact with an oxygen bubble rather than the silicate melt. This occurs when the oxygen produced at the anode fails to escape upward as fast as it is produced. Solutions to this problem are discussed below in the section labeled "Bubble formation and frothing in the melt". Because it is impossible to keep the Pt completely free of oxygen (since the oxygen is being produced there), some oxidation of the Pt is inevitable. We have reported previously (Colson and Haskin, 1992) that the Pt anode appears to be stabilized dynamically by being continuously oxidized and reduced. Whether this oxidation-reduction process destroys the anode over long periods of time remains to be seen. The second cause of Pt anode deterioration is mixing of cathodic metal to the anode, causing it to melt, lose its shape, and incorporate silicate melt (as seen in *Figure 5*). This latter cause of deterioration also greatly decreases the efficiency of oxygen production. Solutions to this problem are discussed below in the sections "Anode-cathode distance" and "Cell potential".

Bubble formation and frothing of the melt:

As we have reported previously (Colson and Haskin, 1992), frothing of the melt is one of the primary causes of energy inefficiency. We identify two causes of frothing: 1) failure of oxygen formed at the anode to escape and 2) formation of Mg gas at the cathode. The latter of these is discussed below in the section "Cell potential". The former depends on the composition of the silicate melt in the cell, the current density of the cell, and the design and orientation of the anode. We have reported previously that SiO2 and Al2O3 concentrations in the melt must be kept low (Colson and Haskin, 1992). This observation is confirmed in these experiments in which high Al2O3 experiments (run in alumina containers) resulted in runaway frothing at current densities corresponding to <0.05A/cm2 cross-sectional area of the container, whereas low Al2O3 experiments (run in spinel containers) did not have runaway frothing at least to 0.2A/cm2. In addition, cell resistance in the low Al2O3 experiments was comparable to that in the high Al2O3 experiments even though the current density in the low Al2O3 experiments was 4-times higher and the anode-cathode distance was 3 times greater (1.5cm in the low Al2O3 experiments, 0.5cm in the high Al2O3 experiments). These differences can be seen by comparing experiments Elecss2L-O to Elecs2R-T in the appendix.

Of equal importance, but somewhat harder to quantify, is the design of the anode. Depending on subtle differences in the shape and orientation of the anode, we have observed several different frothing behaviors: 1) low resistance (few bubbles adhering to the anode) at low current density, with cell resistance increasing to very high values once some threshold current density is reached. We believe this is caused by frothing, i.e. formation of bubbles that do not coalesce or escape from the melt. 2) A cyclic variation in resistance, with a gradual increase in resistance up to a threshold value at which a very rapid increase in resistance to very high values is followed by a rapid decrease to the low value of the cycle. We believe this is caused by the gradual growth of one bubble (or a few) caught underneath the anode which eventually escapes once it reaches sufficient size. 3) A relatively stable cell resistance which is much higher than melt conductivity would suggest it should be. We believe this is caused by a "steady state" number of bubbles clinging to the Pt anode or "perched" bubbles as was observed in Elecss2M (shown schematically in *Figure 6*).

The relative severity of these problems depends on fairly subtle differences in the anode configuration. However, some consistent dependencies on the design can be extracted. *Figure 7* illustrates various anode designs and resultant cell resistances. A general observation is that fewer, larger gaps in the anode are better than more, smaller gaps. In fact, higher currents can often be

achieved by smaller anodes because of the resulting greater space for bubbles to escape. Thus, in this report we use current density relative to the cross-sectional area of the container rather than relative to the anode surface area itself.

Cell potential:

Constraints on cell potential include 1) current density constraints discussed above 2) lower-potential limit set by the need to reduce Si as well as Fe, and 3) upper-potential limit set by the need to avoid producing Mg gas.

Current density in general should be maximized, within the constraints of potential discussed below, by maintaining the melt composition at low $SiO_2 + Al_2O_3$ concentrations and optimizing the design of the anode so that bubble formation and frothing do not greatly increase cell resistance as current density increases. Because reaction kinetics are fairly fast (Haskin et al. 1992), current density is limited primarily by the rate at which reduction components are transported to the electrodes. Thus, keeping "fresh" silicate mixed to the electrodes is important. We observe strong compositional gradients in the silicate melts of our experiments, consistent with minor depletion of FeO and SiO_2 in the vicinity of the cathode. However, because SiO_2 and FeO are major constituents of the melt, sufficient $FeO + SiO_2$ always remains available for reduction. In the worst case of our experiments (Elecss2N, in which the potential was sufficiently high to reduce nearly all constituents of the melt), FeO is completely depleted in the vicinity of the cathode, and SiO_2 concentration is decreased but still comprises nearly 37% of the total melt near the cathode. Although this decrease in concentration results in a slight increase in the potential required to reduce SiO_2, the effect of this depletion on energy efficiency is insignificant relative to other effects.

Si must be reduced as well as Fe, otherwise solid Fe dendrites form (at T below the Fe melting point only) that eventually short the cell. The potential needed to reduce Si in addition to Fe is about 1.4-1.5 volts in excess of the IR potential (in air). Iron dendrites formed in experiment Elecss2O, run at about 1.33 volts in excess of IR potential, are shown in *Figure 8*. These dendrites form complex "bubble-like" patterns in the silicate melt, with the interiors of the bubbles reduced relative the exteriors. Some of these "Fe bubbles" are void after the experiment, suggesting they were filled by some gas during the electrolysis. We do not know the identity of this gas and offer no explanation for why the bubble interiors are reduced relative to the exteriors.

If the potential becomes sufficiently large (about 1.8 volts in excess of IR potential in air) Mg gas

is produced. This gas rises through the melt reacting to form MgO and Fe+Si. The Fe+Si so formed exists as very small beads (~1micrometer and less) that remain in suspension in the melt and mix to the anode, decreasing efficiency and destroying the anode if in sufficient quantity. In addition, although the gas reacts away before it has risen more than a few millimeters through the melt, it creates a bubble horizon between the anode and cathode that greatly increases cell resistance. For these reasons, potential should be maintained such that Mg gas is not produced in significant amounts. *Figure 5* illustrates the distribution of Mg bubbles in Elecss2N, run at 1.8 volts in excess of IR potential.

Anode-cathode distance:

We have reported previously (Haskin and Colson, 1992) that anode-cathode distances on the order of 0.5-1 cm are desirable in order to minimize cell resistance and thus energy lost to resistive heating. However, such small distances may be physically difficult to achieve in a large cell. We have now identified additional reasons to maintain a larger anode-cathode distance. In our experiments, the interface between the metal and melt is sufficiently turbulent that Fe-Si metal beads, whose density differs very little from that of the melt, can become suspended in the melt (see *Figure 5*). These metal beads can get mixed to the anode, causing both deterioration of the anode and a large decrease in oxygen production efficiency when Fe and Si, rather than oxygen, are oxidized at the anode. We have not observed this to occur where the cathode-anode distance is >1cm.

We have done electrolysis experiments with anode-cathode distances in the 1.5-2cm range. Cell resistance is still sufficiently low that high energy efficiency is attained, as discussed below in the section "Energy efficiency".

A second cause of mixing of metal to the anode is related to very small (~1micrometer) metal beads suspended in the melt. These have also only been observed <1cm from the cathode, but because of their small size could presumably be mixed throughout the melt. We believe these are formed by Mg gas (see "cell potential" above) and so can be largely avoided.

Oxygen efficiency:

We have predicted previously how oxygen production efficiency should vary as a function of concentration of divalent iron in the melt. For our experiments, these efficiencies should be between about 65 and 85 % (FeO is about 2-3% of silicate melt). For two experiments, observed efficiencies

(as estimated by metal produced) are much lower than predicted, being in the range of 11-16%. Metal produced was estimated by both petrographic/analytical estimates and by mass-balance calculations based on initial and final melt compositions. In the two experiments with lower-than-predicted efficiencies, metal was mixed to the anode either due to dendrite formation at too low potentials (Elecss2O) or formation of small metal beads by Mg gas at too high potentials (Elecss2N). We believe that the difference in predicted versus observed efficiencies in these experiments is due primarily to mixing of cathodic metal to the anode. This interpretation is supported by the results of Elecss2P, in which oxygen production was measured continuously by a Y-stabilized zirconia electrolyte sensor during electrolysis too short to allow much mixing of cathodic metal to the anode. Measured efficiency for this experiment is 50-60% as shown in *Figure 9*. Expected efficiency is about 70%. In an experiment at intermediate potentials (Elecss2M), oxygen production was estimated based on oxidation of a Ni wire above the cell and oxidation of divalent Fe in the melt above the anode. In this experiment, oxygen production + oxidized iron matched closely that expected, suggesting that metal mixing to the anode was an insignificant problem at the intermediate potentials.

We conclude that efficiencies will approach those we have predicted previously if mixing of cathodic metal to the anode is minimized by increasing anode-cathode distances and if cell potentials are maintained in the range where both Fe and Si are produced, but Mg gas is not produced.

Energy efficiency:

As shown in the appendix, energy efficiency for electrolysis is quite high for the cases in which mixing of cathodic metal to the anode is insignificant. For example, in Elecss2T, with a spinel container and a low-SiO_2, Al_2O_3 melt, potential in the range where Fe and Si but not Mg gas are produced, cathode-anode distance of about 1.5cm, and current density of 0.22A/cm2 (cross-sectional area of container), energy used is only about 3.4 times the theoretical energy to reduce SiO_2.

References

Colson, R. O. (1990) Characterization of metal products of silicate melt electrolysis. Lunar and Planetary Science XXI, Lunar and Planetary Institute, Houston, p 214-215.

Colson R. O. and Haskin L. A. (1990) Lunar oxygen and metal for use in near-earth space: Magma electrolysis. In Engineering, Construction, and Operations in Space II, ASCE, NY, p 187-196.

Colson R. O. and Haskin L. A. (1992) Producing oxygen by silicate melt electrolysis, In Resources

of Near-Earth Space (Ed. J. Lewis) Univ Ariz Press (in press).

Harris, J. H., Grassali R. K., Tenhover A. M., and Ward M. D. (1985) Electrolytic processes employing platinum based amorphous metal alloy oxygen anodes, Eur. Pat. Appl. EP 164,200.

Haskin L. A., Lindstrom D. J., Semkow K. W., and Lewis R. H. (1986) Lunar soil and rock as a source for propellant and constructional materials in space. McDonnell Center for the Space Sciences Report TEL-107, 29p.

Haskin L. A., Colson R. O., Lindstrom D. J., Lewis R. H., and Semkow K. W. (1992) Electrolytic smelting of lunar rocks for oxygen and iron. In Lunar bases and space activities of the 21st century, Lunar Planetary Inst, Houston (in press).

Haskin L. A. and Colson R. O. (1992) Steady state composition with low Fe2+ concentrations for efficient O2 production by "magma" electrolysis of lunar soils. In Engineering, Construction, and Operations in Space III, ASCE, NY p. 651-665.

Lindstrom D. J. and Haskin L. A. (1979) Electrochemical preparations of useful material from ordinary silicate rocks. Proc. Princeton Conf. Space Manufact., AIAA, 3, p129-134.

Lyman T. (ed) (1973) Metals handbook 8th edition Vol. 8 Metallography, structures, and phase diagrams, Am Soc. Metals, Metals Park, Ohio, 466p.

Figure 1. Design for Elecss2E-Elecss2K.

Figure 2. Design for Elecss2L-Elecss2O. Experiments Elecss2P-Elecss2Q are analogous exept spinel rather than alumina is used to contain the silicate melt.

Figure 3. Design for Elecss2P-Elecss2Q.

Figure 4. Beading of Fe-Si molten alloy in silicate melt.

Figure 6. Schematic diagram of Elecss2M, showing gas bubble perched below anode.

Figure 7.

Figure 5. Elecss2N, schematic diagram and backscattered electron image.

Figure 8. Elecss2O, cathode at bottom, anode is at top.

Figure 9. Measured oxygen production rate versus current in Elecss2P.

APPENDIX

Summary of "Scaling-up" Experiments

First Set: Elecss1-Elecss2
Set-up: Pt crucible, Pt wire anode, Ir wire cathode (both inserted from the top as straight wires), T=1480-1490 | C, CO2 atm., 1.9g of SS + 5.6% A12.

Example experiment: Elecss2

Experiment duration=	4min 44sec
Cell potential=	2.4 to 9.8 volts
Ean-Eca=	1.4 volts
current=	0.18 amps
amp-sec=	49.3 coulombs
current density=	4 amps/cm2 (anode surface area)
expected efficiency=	>85%
expected oxygen produced=	0.0035 grams
energy/energy to split SiO2	
if 100% efficiency=	8.5

Observations: Violent frothing of melt results in dramatic increase in cell resistance; where cathode touched Pt crucible the Pt melted, indicating presence of Si.

Second Set: Elecss3-Elecss6
Set-up: Spinel crucible, Pt wire anode, Ir wire cathode (both inserted from the top as straight wires, distance between electrodes ~0.4cm), T=1480 | C, CO2 atm., 0.64g of SS + 5.6% A12.

Example experiment: Elecss6

Experiment duration=	30min 33sec
Cell potential=	2.3 volts
Ean-Eca=	1.45 volts

current= 0.023 amps
amp-sec= 41.6 coulombs
current density= 0.15 amps/cm2 (anode surface area)
expected efficiency= >85%
expected oxygen produced= 0.0035 grams
energy/energy to split SiO2
if 100% efficiency= 2.16

Observations: Frothing ~ doubled cell resistance; Fe+Si observed at cathode; Spinel crucible survived >2hrs in contact with melt with no signs of corrosion; Spinel precipitated at the cathode; Ir cathode deteriorated leaving a black cloud of submicron sized Ir particles in vicinity of cathode.

Third Set: Elecss7-Elecss17
Purpose: Study effect of anode configuration (e.g. straight wire vs coils of varying "tightness", Pt screen, moving anode up and down, anode at different depths in melt, etc.) on resistance increase caused by frothing.
Set-up: Spinel crucible, Pt wire anode, Pt wire coil cathode entering through a hole in the bottom of the crucible, electrodes ~ 0.5cm apart, T=1490 | C, CO2 atm., ~0.5g of SS + 5.6% A12.

Example experiment: Elecss14
Experiment duration= 5min 43sec
Cell potential= 1.2-3.4 volts
Ean-Eca= 0.8 volts
current= 0.04 amps
amp-sec= 13.7 coulombs
current density= 0.3 amps/cm2 (1/2 anode surface area)
current density= 0.08 amps/cm2 (crucible x-sectional area)
expected efficiency= >85%
expected oxygen produced= 0.00097 grams
energy/energy to split SiO2
if 100% efficiency= 1.88
energy/energy to split FeO
if 100% efficiency= 3.36
Observations: Main variable affecting frothing is current density relative to cross sectional area of crucible, other variable of minimal effect. Resistance increases progressively and ultimately sample is lost from crucible due to frothing for all configurations and current densities (<0.015 to >0.3A/cm2).

Fourth Set: Elecss2A-Elecss2D
Set-up: Spinel crucible, Pt wire coil anode (0.02" dia), Pt wire coil cathode (0.04" dia) entering through a hole in the bottom of the crucible, electrodes ~ 0.5cm apart, T=1490 | C, CO2 atm., ~1.29g of SS2 + 4.8% A12 (SS2 is lower in SiO2 and Al2O3 than SS).

Example experiment: Elecss2D
Experiment duration= 37min 21sec
Cell potential= 0.92 volts
Ean-Eca= 0.8 volts
current= 0.025 amps
amp-sec= 58.5 coulombs
current density= 0.2 amps/cm2 (1/2 anode surface area)
current density= 0.06 amps/cm2 (crucible x-sectional area)

expected efficiency= >85%
expected oxygen produced= 0.0041 grams
energy/energy to split SiO2
if 100% efficiency= 0.87
energy/energy to split FeO
if 100% efficiency= 1.55

Observations: Frothing in this composition does not get out of hand if current density is < ~0.2A/cm2, otherwise resistance increases rapidly until sample froths out of container. Gas appears to be generated at the cathode. Pt is mobile in cathode vapor bubbles. Anode is reacting (oxidizing?) during electrolysis but appears to not migrate far before Pt-oxides are reduced by the melt. Spinel crucible failed near the cathode, perhaps due to reaction with cathodic vapor.

Fifth Set: Elecss2E-Elecss2K
Set-up: Spinel crucible held in a steel container, molten (Zn,Ni), (Ni), or solid Pt cathode connection through a hole in the bottom of the crucible to the steel container, Pt wire coil anode inserted from the top, electrodes ~ 0.5cm apart, T=1440-1450 | C, Argon atm., ~0.4 to 1g of SS2 + 5-13% A12.
General observations: Combination of failure (melting) of steel when in contact with the cathode product, solubility of Argon in metal product, vapor formed by degassing of steel, tendency of molten metal to bead, and tendency of molten metal to not make an electrical connection through a small hole in the bottom of the crucible make this configuration unsuited for the long-term electrolysis experiments and simulation of a "real" working cell for which it was intended. Metal has high surface energy with both silicate melt and spinel crucible; 0.7cm "cliffs" are possible (FeSS2) suggesting that on the scale of 0.5cm (necessary electrode separation) this may be a problem.

Example experiment: Elecss2l
Experiment duration= 27min 38sec
Cell potential= 1.25 volts
Ean-Eca= 0.9 volts
current= 0.023 amps
amp-sec= 43 coulombs
current density= 0.065 amps/cm2 (crucible x-sectional area)
expected efficiency= 68%
expected oxygen produced= 0.0024 grams
energy/energy to split SiO2
if 100% efficiency= 1.47
energy/energy to split FeO
if 100% efficiency= 2.63

Observations: Connection between molten pool and steel container was not achieved, so current flow is through the narrow silicate melt "neck" drilled in the bottom of the crucible; molten metal appeared to "float" up from bottom of crucible and to bead strongly.

Sixth Set: Elecss2La,b-Elecss2O

Set-up: Experiment contained in an alumina tube (inside dia ~ 0.8-0.9cm); cathode is steel rod inside tube stabilized by T gradient (extends to cool parts of furnace ~1100-1200 | C); anode is Pt coil inserted from top of tube, T=1440 | C; Argon atm.; In Elecss2L,N,O the glass is exposed to air and the steel rod to Argon; In Elecss2M the glass is sealed from air and a package of Ni metal is suspended over the melt to "capture" escaping oxygen. 4-5.3g of SS2 + 10-13%A12 in L and M; ~2g SS2+10% A12 plus ~0.2g A12 added in increments in N and O.

Example experiment: Elecss2Lb

Experiment duration= 28min 31sec
Cell potential= 2.77 volts
Ean-Eca= 1.45 volts
current= 0.094 amps
amp-sec= 167.7 coulombs
current density= 0.15 amps/cm2 (crucible x-sectional area)
current density= 0.22 amps/cm2 (1/2 Pt anode area)
expected efficiency= 69%
expected oxygen produced= 0.01 grams
energy/energy to split SiO2
if 100% efficiency= 3.21

Observations: Amount of metal produced ~ that expected on basis of current if all product is Fe; Frothing extended glass ~7cm (factor of 3 to 4) up alumina tube beyond where it was expected to extend. Both Si and Fe produced.
Note: design permits new feedstock to be introduced periodically from top of alumina tube, permits anode to be raised or lowered during the experiment, and an oxygen getter can be attached to top of alumina tube to measure oxygen production.

Example experiment: Elecss2M

Experiment duration= 1hr 29min 18sec
Cell potential= 2.14 volts
Ean-Eca= 1.34 volts
current= 0.05 amps
amp-sec= 267.9 coulombs
current density= 0.085 amps/cm2 (crucible x-sectional area)
current density= 0.139 amps/cm2 (1/2 Pt anode area)
expected efficiency= 74%
expected oxygen produced= 0.016 grams
observed oxygen production:
Oxygen trapped in Ni above cell 0.0034g
Oxygen in Fe2O3 in glass (assuming all Fe above anode is oxidized) 0.0112g
energy/energy to split SiO2
if 100% efficiency= 2.31

Observations: No indication that alumina tube is failing; periodic (4 to 8 min) increase then rapid decrease in resistance due to accumulation of bubbles under anode; presence of bubbles generated near the cathode; Fe above anode was oxidized by oxygen produced suggesting that good effeciency requires a low percentage of total melt be above the anode. Metal produced is mostly Fe forming partially oxidized dendrites and plating the steel cathode. The Pt anode is oxidized where it contacts gas (O2) bubble but is not oxidized where it is in contact with melt.
Note: experiment is closed, products can be quatitatively accounted for.

Example experiment: Elecss2N

Experiment duration= 8hrs 15min (2hrs 24min)
Cell potential= 1.3 - 15 V (2.6 V)
Ean-Eca= 1.2 - 2.3 V (1.8 V)
current= 0.034 - 0.095 A (0.034 A)
amp-sec= 1227 C (294 C)
current density (crucible x-sectional area)= 0.05-0.16 A/cm2 (0.06)
current density (1/2 Pt anode area)= 0.1-0.3 A/cm2 (0.104)
expected efficiency= 75%
calculated efficiency (from metal produced)= 16%
metal produced= calculated O2
Si: 0.0108g 0.0123g
Fe: 0.0096g 0.00274g
Ti: 0.00088g 0.00059g
Mn: 0.00014g 0.00004g
Cr: 0.00028g 0.00013g
calculated oxygen produced= 0.0158 grams
energy/energy to split SiO2 17 (12)
energy/energy to split SiO2
if 100% efficiency= 2.6 (1.8)

(Values in parentheses are for the last 2.5 hrs of electrolysis where cell resistance was lowest because of anode design and current density.)

Observations: Substantial Al2O3 dissolves into the melt from the container, increasing viscosity and resistivity and causing spinel to precipitate on the cell wall. Efficiency << expected because of mixing of metal to the anode, observed in periodic decrease in Ean-Eca (as metal mixed to the anode is reoxidized), deterioration of the anode (causing it to melt and mix with silicate melt), observed suspended metal particles, and mass balance calculations indicating that SiO2 and FeO are increased in concentration near the anode. Bubbles at bottom of cell may be Mg (g) (potential is sufficiently high). This Mg would quickly back-react with the melt reducing Fe etc. and, in fact, there is a distinct boundary at the line of bubbles (Fe-poor below line). These bubbles increase cell resistance and mix metal to the anode and may also cause the formation of submicron-sized metal particles (seen in sample in vicinity of bubble line) that remain in suspension and eventually mix to the anode. Thus, the upper potential limit may be where Mg (g) begins to form. Periodic addition of feedstock during the experiment results in periodic decrease in cell resistance, apparently due to "clearing" of bubbles from the anode; there is no concurrent decrease in the potential required to get a given current. "Stirring the melt by moving the anode up and down does not decrease resistance and in some cases increases it. In addition, stirring mixes more metal to the anode causing reduced efficiency (as evidenced by change in cell potential at constant current). The effect of anode design is discussed after expt Elecss2O.

Note: Compositional maps of the quenched sample combined with periodic sampling of the melt during the experiment combine to permit mass-balance calculations to be made of products (spinel, melt, residual melt) and the amount of Al2O3 added from the cell wall. Metal composition was also determined by direct microprobe analyses and amount was estimated from diffusion profiles in the cathode and point-counting of metal suspended in melt.

Example experiment: Elecss2O

Experiment duration= 5hrs 50min
Cell potential= 1.5 - 3.1 V (2 V)
Ean-Eca= 1.28 - 1.48 V (1.33 V)
current= 0.034 A
amp-sec= 722 C
current density (crucible x-sectional area)= 0.057 A/cm2
current density (1/2 Pt anode area)= 0.104 A/cm2
expected efficiency= 80%
calculated efficiency (from Fe produced)= 11%
metal produced= calculated O2
Fe: 0.0232g 0.00663g
calculated oxygen produced= 0.00663 grams
energy/energy to split FeO 12.3
energy/energy to split FeO
if 100% efficiency= 1.7

(Values in parentheses are mean values for experiment)
Observations: Substantial Al2O3 dissolves into the melt from the container, increasing viscosity and resistivity and causing spinel to precipitate on the cell wall. Efficiency << expected because of mixing of metal to the anode causing a decrease in Ean-Eca to ~0.1-0.4V lasting ~15 min in one case as the metal oxidizes. This amount of metal-cycling (that observed to occur in a few distinct events) cannot account for all the decreasee in efficiency, and it is likely there is also a continuous feed of metal to the anode. Stirring by moving the anode up and down appears to exacerbate this problem. Adding new A12 does not appear to clear bubbles from the anode as it did in Elecss2N, although the bubble problem is less significant than in that experiment. Progressive increase in cell resistance is likely due Al2O3 dissolution into the melt. The cell shorted when Fe dendrites connected electrodes. Product metal was Fe (solid), as expected from Ean-Eca potential. These dendrites formed "bubbles" filled by either glass or gas of unknown origin. The glass on the interiors of the "bubbles" appears more reduced than on the exterior, as in A12-1cg.
Note: Fe metal produced was calculated by mass balance.

Anode design effects (from Elecss2N unless noted, ~same anode surface area unless noted, first value is cell resistance in ohms 10 minutes after start of electrolysis at 0.049A, second value where given is a 'steady state' cell resistance at 0.049A, the third value where given is the 'steady state' cell resistance at 0.034A). Summary: fewer large spaces are better than more small spaces in anode.

92.4 >92.4 42

69.8 80 <70
(SA ~25% more than others)

60.2 68 >45

38 68 21

18 >18 22
from Elecss2O

Seventh Set: Elecss2P-Elecss2Q
Set-up: Experiment contained in an spinel tube (inside dia ~ 1.6cm) couched inside an alumina crucible; cathode is a steel rod inside the crucible and bottom part of the spinel; anode is Pt coil inserted from above, T=1440 | C; Argon atm.; Oxygen produced is measured continously by a yttria-stabilized zirconia electrolyte oxygen sensor inside the furnace a few inches below the experiment. 8.9 grams glass is 10% A12, 90% "steady state".

Example experiment: ElecssP

Experiment duration= 5 min
Cell potential= 4 volts
Ean-Eca= 1.46 volts
current= 0.25 amps
current density= 0.12 amps/cm2 (crucible x-sectional area)
current density= 0.24 amps/cm2 (1/2 Pt anode area)
expected efficiency= 67%
measured efficiency= 63%
energy/energy to split SiO2
if 100% efficiency= 4.1

Observations: Oxygen produced varies with current as expected (see Fig.??). Short duration of experiment due to failure of the alumina crucible along fractures formed during a previous heating and quenching cycle.

Eighth Set: Elecss2R-Elecss2T
Set-up: analogous to Sixth Set except used spinel rather than alumina tubes and electrodes ~1.5cm apart rather than ~ 0.5cm apart. Cell is exposed to air. 4-8 grams glass added is 12% A12, 88% "steady state".

Example experiment: ElecssR

Experiment duration= 30min (ran longer)
Cell potential= 3.4 (1.5-5.5) volts
Ean-Eca= ~1.2 volts
current= 0.06 (0.056-0.072) amps
current density= 0.11 amps/cm2 (crucible x-sectional area)
current density= 0.17 amps/cm2 (1/2 Pt anode area)
expected efficiency= 75%
energy/energy to split SiO2
if 100% efficiency= 3.0

Observations: Substantial melt (more than half) goes into porous spinel, porous spinel is structurally weak, need denser spinel. Periodic gradual increase in resistance up to 74 ohms or so followed by rapid decrease to 13 ohms or so (resistances are avgs over 27 seconds), presumably as a bubble grows between the anode and cathode, then escapes. (The anode ring was attached to the lead such that Pt wires partially blocked the space in the center of the ring, possibly explaining difficulty for bubbles to escape).

Example experiment: ElecssT

Experiment duration= 12 min (ran longer)
Cell potential= 3.8 volts
Ean-Eca= 1.42 volts
current= 0.116 amps

current density= 0.2 amps/cm2 (crucible x-sectional area)
current density= 0.2 amps/cm2 (1/2 Pt anode area)
expected efficiency= 75%
energy/energy to split SiO2
if 100% efficiency=n 3.4

Observations: Porous spinel is structurally weak, need denser spinel. No indication of significant frothing up to maximum applied current density (0.2A/cm2).

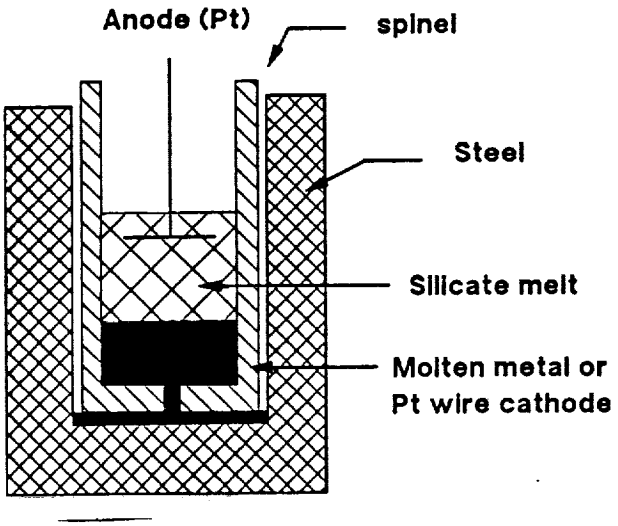

Fig. 1 Design for Elecss2E-Elecss2K.

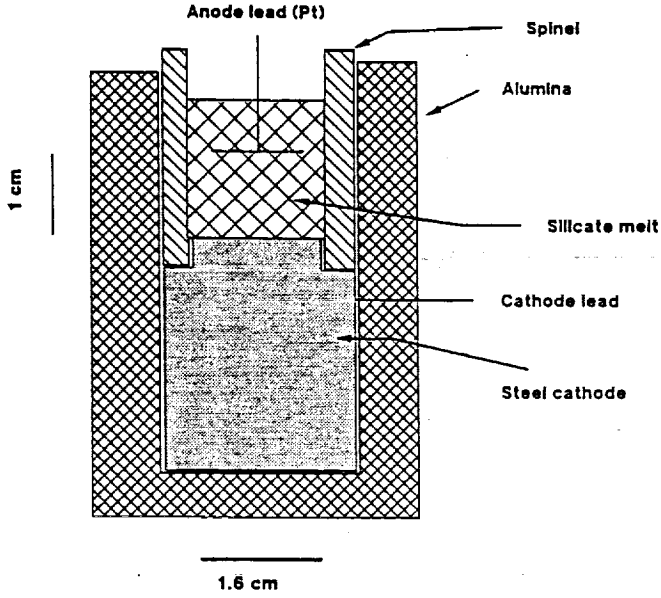

Fig. 3 Design for Elecss2P-Elecss2Q.

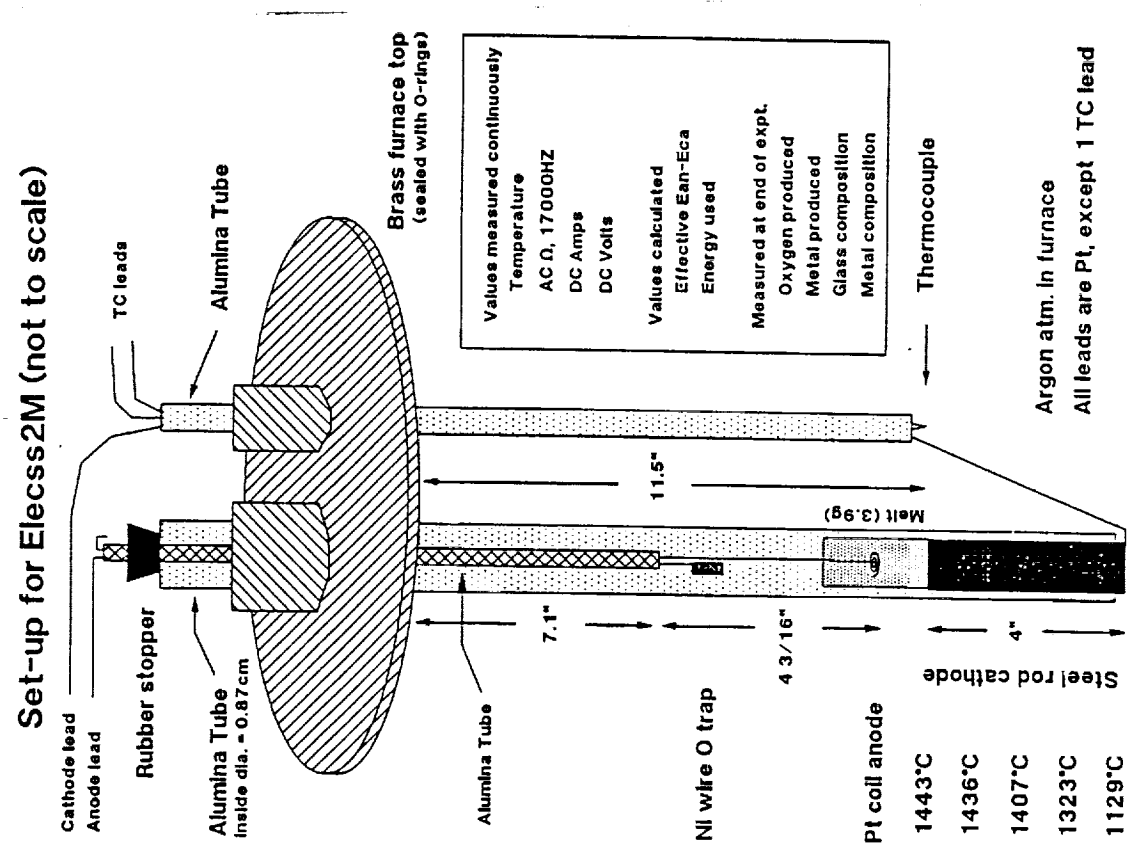

Fig. 2 Design for Elecss2L-Elecss2O. Experiments Elecss2P-Elecss2Q are analogous exept spinel rather than alumina is used to contain the silicate melt.

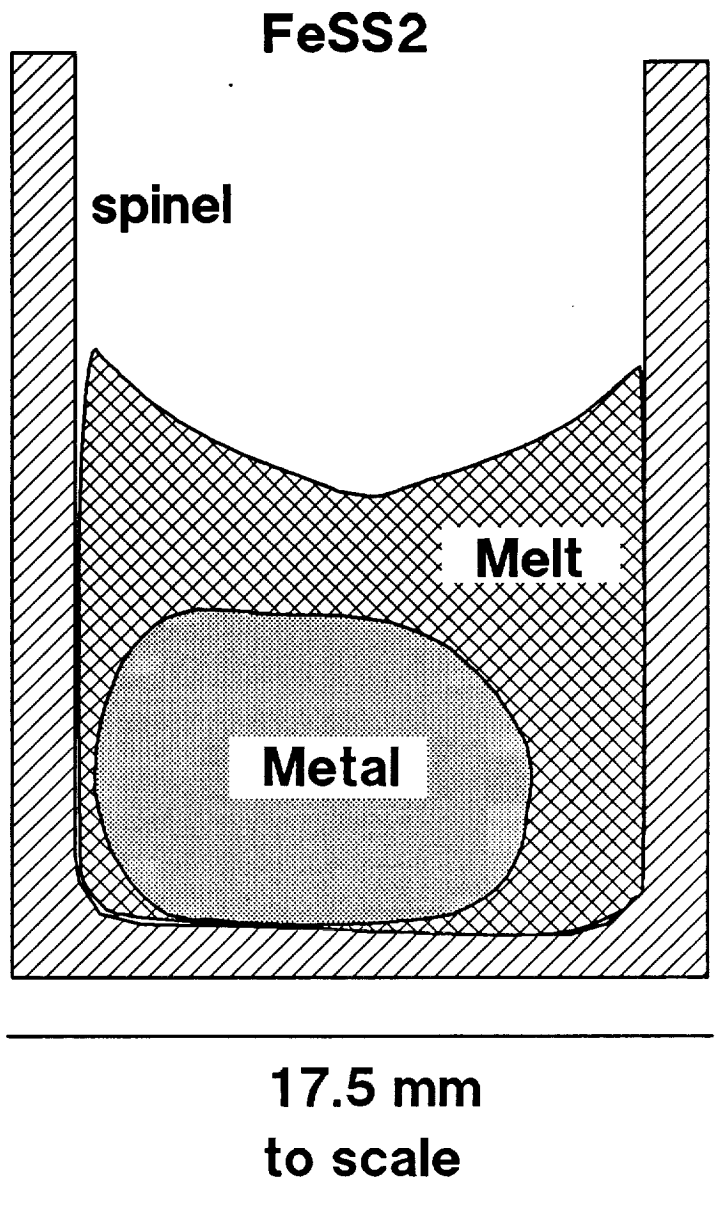
FeSS2
spinel
Melt
Metal
17.5 mm
to scale

Fig. 5 Elecss2N, schematic diagram and backscattered electron image.

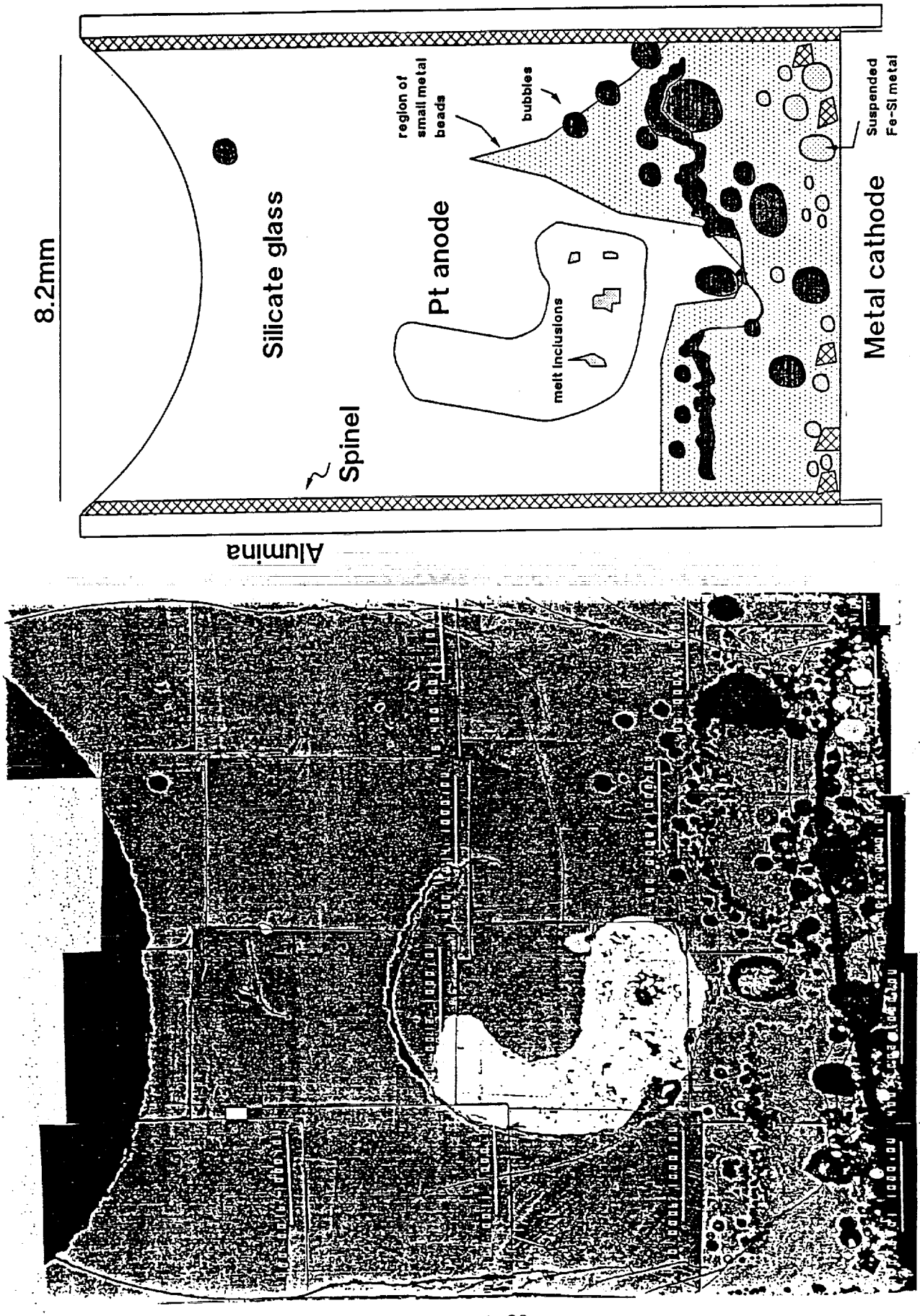

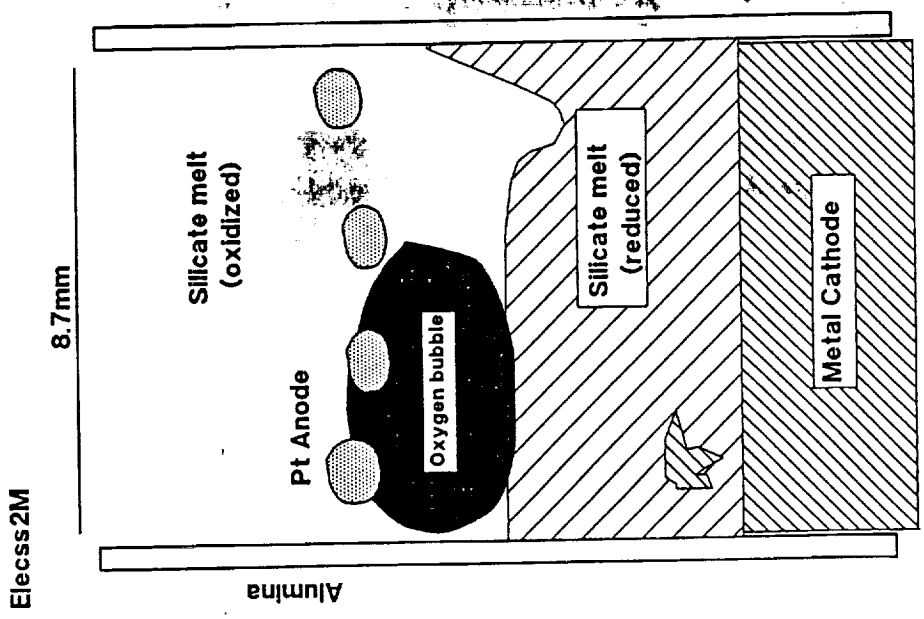

Fig. 6 Schematic diagram of Elecss2M, showing gas bubble perched below anode.

Effect of Anode design on cell resistance increase due to frothing[1]

	Resistance after 10min at 0.049A	Resistance after >> 10min at 0.049A	Resistance after >> 10min at 0.034A	
	92.4	>93	42	Elecss2N
	69.8	80	<70	Elecss2N [2]
	60.2	68	>45	Elecss2N
	38	68	21	Elecss2N
	18	>18	22	Elecss2O

Summary: Fewer bigger holes are better than more littler holes.

1 Cell parameters such as electrode separation, melt composition etc. are approximately the same.

2 Anode surface area ~25% greater than for other anodes.

Fig. 7.

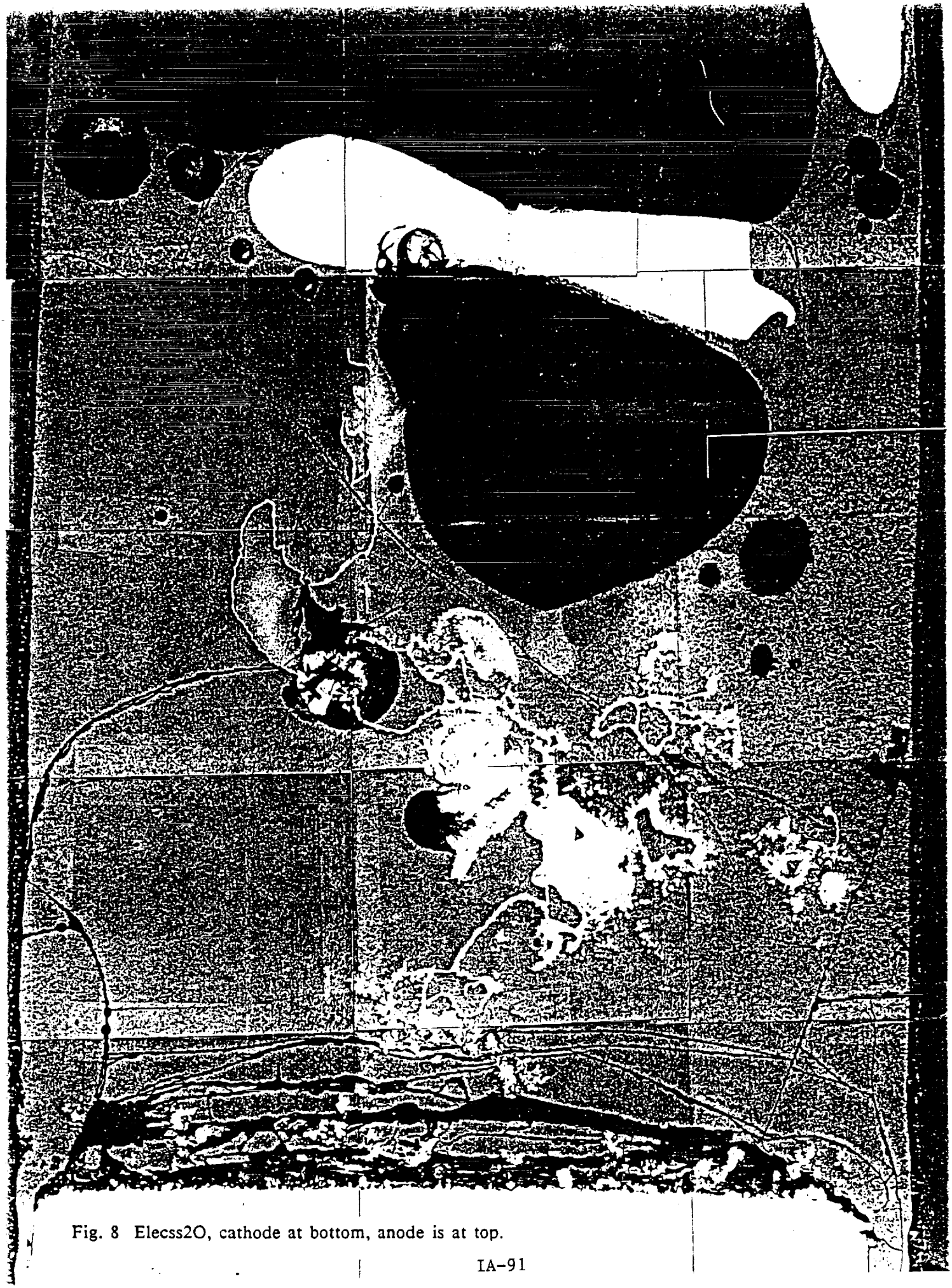

Fig. 8 Elecss2O, cathode at bottom, anode is at top.

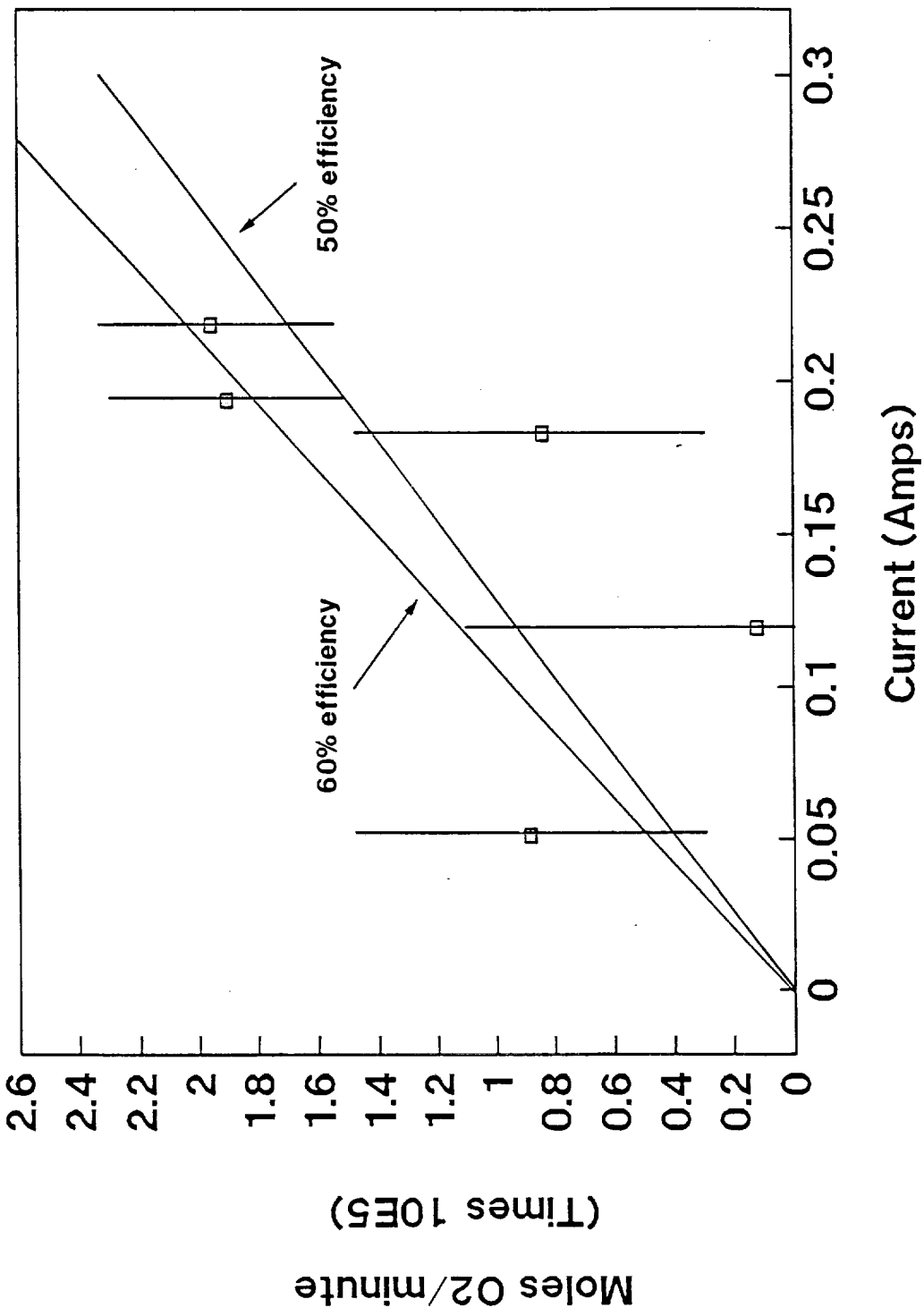

Fig. 9. Measured oxygen production rate versus current in Elecss2P.